scientific reports

Check for updates

OPEN

Synergistic antibacterial activity of curcumin and phage against multidrug-resistant *Acinetobacter baumannii*

Sujintana Janesomboon[1], Thanchanok Sawaengwong[1], Veerachat Muangsombut[1], Muthita Vanaporn[2], Pitak Santanirand[3], Kanyanan Kritsiriwuthinan[4], Ozan Gundogdu[5], Narisara Chantratita[2,6], Janet Yakubu Nale[7], Sunee Korbsrisate[1] & Patoo Withatanung[1]✉

Acinetobacter baumannii **is a priority bacterial pathogen and leading cause of nosocomial infections, particularly in intensive care units (ICUs). The average incidence of carbapenem-resistant *A. baumannii* infections in ICUs is 41.7 cases/1,000 patients, highlighting the urgent need for more effective alternative therapies to replace carbapenems. Thus, this study aimed to investigate for the first time the antibacterial activity of curcumin in combination with the novel phage vB_AbaSI_1 to combat multidrug-resistant (MDR) *A. baumannii* in vitro. Phage vB_AbaSI_1 (capsid diameter 91 nm, contractile tail 94/20 nm) was isolated from sewage and infects ~ 29% of the 131 bacterial isolates examined. The 52,783 kb phage genome has 75 ORFs, encodes an integrase, lacks tRNAs/virulence genes, and belongs to the *Caudoviricetes*. Commercially sourced curcumin (400 µg/mL), combined with phage vB_AbaSI_1 (MOI 100) reduced MDR *A. baumannii* 131 to undetectable levels 1 h post-treatment at 37 °C, and this efficacy was further extended for 5 h in double-dosed phage/curcumin-treated cultures. In contrast, treatment with just phage vB_AbaSI_1 reduced bacterial growth but rebounded within 3 h, while curcumin-only treated cultures showed only 1-log bacterial reduction compared to untreated control. The phage/curcumin synergy occurred exclusively with phage-susceptible strains pre-curcumin exposure. This suggests the potential disruption of bacterial cell membrane during phage infection allowing curcumin entry, as no synergy was observed with phage-resistant strains. This innovative strategy of combining phage and curcumin showed great efficacy at controlling MDR *A. baumannii* and has a potential for therapeutic deployment. Future work will focus on engineering the phage to make it therapeutically acceptable.**

Multidrug-resistant (MDR) bacterial infections pose not only a significant global public health threat but also cause a substantial economic loss to the healthcare system. The World Health Organization (WHO) ranked MDR infections as one of the top ten global health threats[1], with an estimated 8.22 million deaths globally projected to be associated with antimicrobial resistance (AMR) by 2050[2]. WHO also identified MDR *Acinetobacter baumannii*, a Gram-negative bacterium, as a critical priority pathogen requiring urgent treatment interventions[1]. A recent systematic review of 22,876 ICU patients from seven Southeast Asian countries revealed that infections due to *A. baumannii* are significantly higher in the region than in other parts of the world[3]. Pertinent to Thailand, *A. baumannii* is a major cause of hospital-acquired infections and responsible for over 15,000 deaths annually[4]. Specifically, the carbapenem-resistant *A. baumannii* (CRAB) accounts for 70–88% of cases[5] indicating its clinical significance in the region. According to the Centers for Disease Control and Prevention (CDC), the incidence of CRAB increased by ~ 78% between 2019 and 2020 in the US[6]. Hence, new alternative therapy for *A. baumannii* is urgently needed because carbapenem is the last-line antibiotic for the infection.

[1]Department of Immunology, Faculty of Medicine Siriraj Hospital, Mahidol University, Bangkok, Thailand. [2]Department of Microbiology and Immunology, Faculty of Tropical Medicine, Mahidol University, Bangkok, Thailand. [3]Department of Pathology, Faculty of Medicine, Ramathibodi Hospital, Mahidol University, Bangkok, Thailand. [4]Faculty of Medical Technology, Rangsit University, Pathum Thani, Thailand. [5]Department of Pathogen Molecular Biology, Faculty of Infectious and Tropical Diseases, London School of Hygiene and Tropical Medicine, London, UK. [6]Mahidol-Oxford Tropical Medicine Research Unit, Faculty of Tropical Medicine, Mahidol University, Bangkok, Thailand. [7]Centre for Epidemiology and Planetary Health, Scotland's Rural College, Inverness, UK. ✉email: patoo.wit@mahidol.ac.th

Phages have been developed as therapeutic agents since the early 1900s in Eastern Europe and the Soviet Union. However, interest in phage therapy declined during World War II, prior to the widespread success of penicillin[7]. Research on therapeutic phages for *A. baumannii* infections has resurged, with recent efforts focusing on isolating novel phages or developing phage cocktails and combining them with antibiotics to specifically target *A. baumannii*[8,9]. Published in vivo phage therapeutic studies for *A. baumannii* have showed promising results. For instance, phage therapy has improved the survival rates and reduced bacterial colonization in zebrafish[10], successfully resolved *A. baumannii*-infected wounds in diabetic rats[11], and lung infections in mice[12]. Despite these successes, clinical data on *A. baumannii* phage therapy is still very limited, with specific paucity of information on potential ways to improve the strategy using other remedies.

Using therapeutic bacteriophages (phages, viruses which specifically infect bacteria) has many advantages such as targeted specificity and preservation of microbial niche. However, bacteria can develop diverse defense mechanisms such as abortive infection, CRISPR-Cas, quorum sensing, and restriction-modification systems to evade phage attack[13]. Therefore, researchers are exploring new ways to enhance the antimicrobial effectiveness of phages to overcome these defense strategies. One such approach is combining phages with other therapeutic agents. For example, phage-antibiotic combinations have demonstrated synergistic antimicrobial effects in a *Galleria mellonella* larval *A. baumannii* infection model[14]. Remarkably, a 42-year-old man who was co-infected with MDR *Klebsiella pneumoniae* and *A. baumannii* was successfully treated with a combination of antibiotics and phages[15].

Besides phage-antibiotic combinations, phage-phyto extract combinations show promising results. For example, combining phages with *Stephania suberosa* roots, *Oroxylum indicum* fruits, and *Boesenbergia rotunda* rhizomes extracts reduced *Escherichia coli* growth by 2–3 log10 within 6 h[16]. Similarly, phage-sacha inchi oil combinations also synergistically controlled MDR *A. baumannii*[17].

One of the most studied spices for antimicrobial activity is turmeric (*Curcuma longa* L.), commonly cultivated in India, Southeast Asia, China, and other tropical regions[18]. Traditionally, turmeric has been a staple in cooking, being used as a spice or a coloring agent in dishes such as curry, and in products like cheese and butter[19]. Among many compounds found in turmeric, curcumin is the major bioactive[20]. Curcumin (1,7-bis(4-hydroxy-3-methoxyphenyl)-1,6-heptadiene-3,5-dione), often referred to as the "wonder drug of life"[21] is a natural polyphenol[22] with a long history of numerous pharmacological applications[23]. Curcumin has been widely recognized for its role in managing inflammatory conditions[24], metabolic syndrome[25], and pain[26]. Much of its efficacy stems from its potent antioxidant and anti-inflammatory properties[27]. Notably, curcumin exhibits broad-spectrum antimicrobial activity for *E. coli*, *Staphylococcus aureus*, *Salmonella* serovar Typhi, *Pseudomonas aeruginosa*, and *A. baumannii*[28]. In addition to its antibacterial effects, curcumin has demonstrated anti-biofilm activity against, and reduced virulence of *A. baumannii* in *Caenorhabditis elegans* infection model[29].

In this study, phage vB_AbaSI_1 was isolated from sewage and tested for its in vitro antibacterial activity and in combination with curcumin against MDR *A. baumannii*. Various treatment parameters were investigated including the multiplicity of infection (MOI-number of infective phage particles exposed to bacteria), single vs. double doses and duration of treatments. The data suggests that the optimized curcumin-phage combination showed synergistic effects, leading to better antibacterial activity against MDR *A. baumannii*. These findings support the potential application of curcumin-phage combination as a promising therapeutic strategy against MDR *A. baumannii* infections and indeed, for other MDR bacterial infection.

Results

Identification of *A. baumannii* strain for optimal phage isolation

To identify the *A. baumannii* strains which carry prophages that may interfere with phage isolation from sewage, the 44 *A. baumannii* strains were treated with mitomycin C (MMC), a known inducer of prophages. As a result, 41 (93.18%) of the strains indicated the release of infecting MMC-inducible phages as evidenced by the formation of plaques against a panel of *A. baumannii* strains (Supplementary Table 1). This 93.18% proportion suggests a high prevalence of prophage carriage within the genomes of the *A. baumannii* strains, that are susceptible to MMC induction.

Of the three strains lacking MMC-inducible prophages, only *A. baumannii* 131 supported phage infection, and formed plaques making this strains the ideal host for phage isolation. However, the possible existence of other prophages in the genome of *A. baumannii* 131 which could not be induced by MMC but may be induced by other agents could not be ruled out, or the possibility that other MMC-induced prophages were released but could not infect the panel of *A. baumannii* host strains here.

A. baumannii phage vB_AbaSI_1: a phage belonging to *Caudoviricetes* and produced transparent halo plaques

From the 100 sewage samples collected across Thailand, 15 *A. baumannii*-specific phages were isolated (15.0% isolation rate) using *A. baumannii* strain 131 as target bacterial host. Phage vB_AbaSI_1 was chosen for further study due to its broader host range, infecting more diverse *A. baumannii* strains than the other isolates. The plaque morphology of phage vB_AbaSI_1 on *A. baumannii* strain 131 showed uniformly clear lysis zone surrounded by transparent halos with a diameter of approximately 2 mm (Fig. 1A). The clear plaques observed indicates effective lytic activity against the *A. baumannii* strains tested and this is critical for our downstream therapeutic analyses. The transmission electron microscopy (TEM) analysis revealed that the structural morphology of the phage vB_AbaSI_1 appeared to have a contractile tail 94/20 and capsid of 91 nm diameter as shown in Fig. 1B.

Phage vB_AbaSI_1 exhibits narrow host-range, short latent period, and large burst size

The host range of phage vB_AbaSI_1 was evaluated by spot assay on a confluent culture of *A. baumannii* 131. As shown in Table 1, phage vB_AbaSI_1 successfully lysed 38 of the 131 (29.01%) *A. baumannii* strains collected

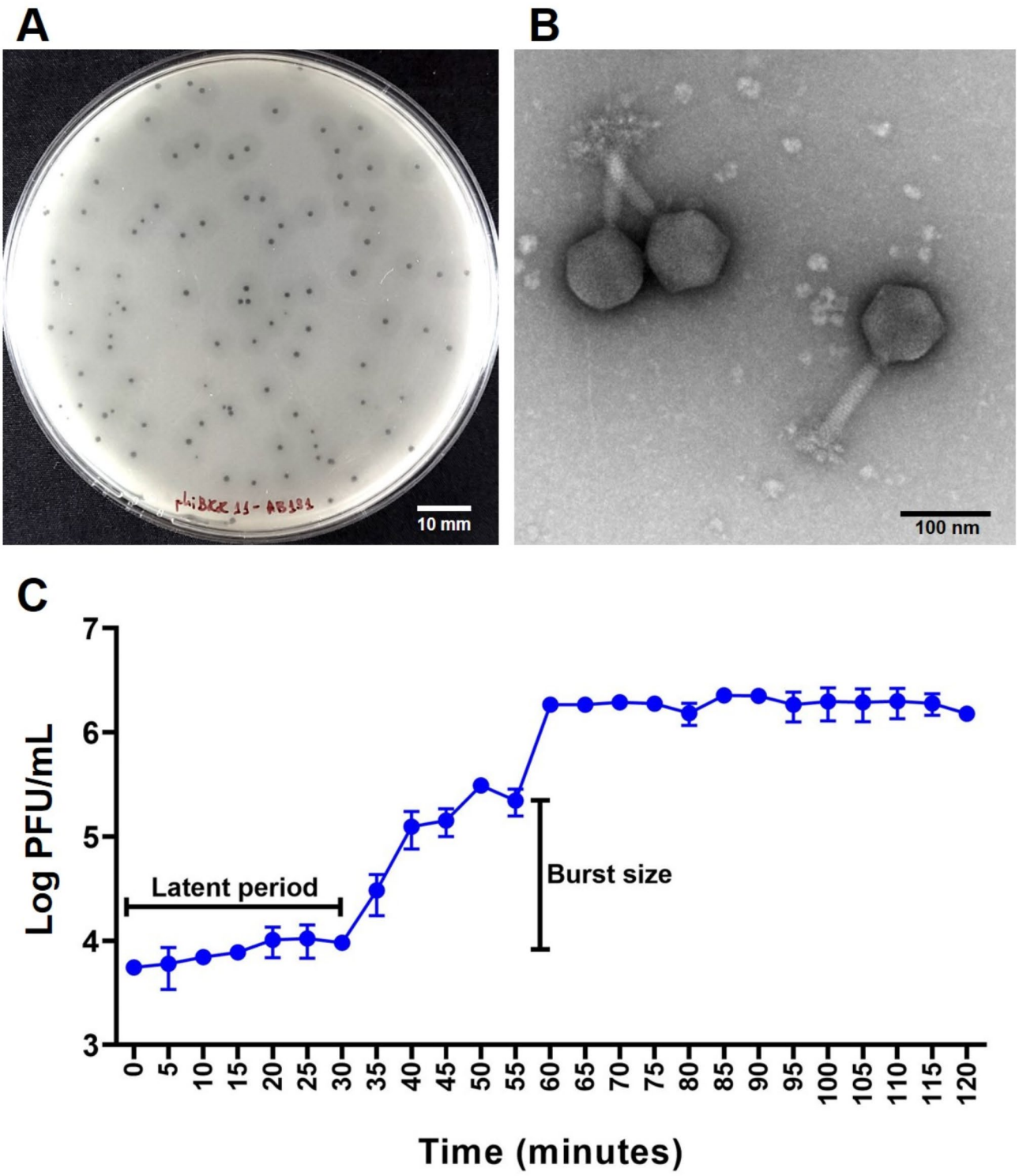

Fig. 1. Morphological and growth characteristics of phage vB_AbaSI_1. (**A**) Plaque morphology on a lawn of *A. baumannii* strain 131. The phage forms clear, well-defined plaques with surrounding halos. (**B**) Transmission electron microscopy image of phage vB_AbaSI_1. The phage has hexagonal capsids along with a long contractile tail. (**C**) One-step growth curve of phage vB_AbaSI_1. Error bars represent standard deviations from three independent experiments.

from Thai patients. However, the phage demonstrated no infectivity towards 35 isolates of other Gram-negative and Gram-positive bacteria, including *K. pneumoniae* (11 isolates), *P. aeruginosa* (10 isolates), *E. coli* (5 isolates), *S. aureus* (5 isolates), and *Burkholderia thailandensis* (4 isolates). This specificity suggests that vB_AbaSI_1 is highly selective for *A. baumannii*, albeit with a relatively narrow host range within this species[30].

Sources of *A. baumannii*	Numbers of isolates	Numbers of positive infection/numbers of isolates (%)
Clinical samples (pus, sputum, urine, blood)	85	27/85 (31.76%)
Catheters	2	0/2 (0%)
Laboratory stock	43	10/43 (23.26%)
Standard strain (ATCC19606)	1	1/1 (100%)
Total	131	38/131 (29.01%)

Table 1. Infectivity of the isolated phage vB_AbaSI_1 against 131 *A. baumannii* isolates gathered from different sources during the years 2014–2021.

To further determine the growth kinetics of phage vB_AbaSI_1, a one-step growth curve analysis was conducted, as illustrated in Fig. 1C. The phage exhibited a latent period of 30 min, which represents the time between phage attachment and the release of progeny phages following replication within the bacterial host. Additionally, the burst size, or the number of phage particles produced per infected bacterial cell, was determined to be 136 plaque-forming units (PFU) per cell.

The relatively short latent period, coupled with a substantial burst size, indicates that this phage is capable of rapidly generating large number of progenies, which is advantageous for timely bacterial clearance in therapeutic applications. These findings highlight the potential utility of phage vB_AbaSI_1 to effectively lyse MDR *A. baumannii*.

A. baumannii phage vB_AbaSI_1 is stable in a wide range of pH and temperatures

Adverse environmental factors may cause a significant decrease in phage infectivity. The stability of the isolated phage vB_AbaSI_1 under different pH was assessed to ensure its optimal stability and delivery. At pH 1, the phage was rapidly inactivated, showing no recoverable viable phage particles immediately upon exposure. At the extreme alkaline condition of pH 13, a significant reduction in viability was observed, with a 4-log decrease in viable phages compared to the control after just 1 h post-treatment. Phages were undetectable after 24 h of exposure to this pH (Fig. S1A). This suggests that the phage is stable in a wide pH range, between 3 and 11. Regarding thermal stability, phage vB_AbaSI_1 exhibited high stability at 4 °C, room temperature (~ 27-30 ºC), and 37 °C, phages were stable for up to 48 h. However, at 45 °C, a significant decrease in phage viability was observed after 24 h, which became more pronounced after 48 h of incubation (Fig. S1B). The inability of the phage to tolerate a temperature of 45 °C concurs with previous reports[31].

Genomic characteristics of phage vB_AbaSI_1: seven functional modules and lysogenic potential

The circular genome map of phage vB_AbaSI_1 is illustrated in Fig. 2. The genome consists of 52,783 base pairs (bp) with a G + C content of 38.02%, a typical composition of phages infecting *A. baumannii*. Genome analysis identified 75 predicted open reading frames (ORFs), with no tRNA genes detected, suggesting that the phage relies entirely on the host machinery for translation. Of these ORFs, 53 were located on the positive strand and 22 on the negative strand. Detailed genome annotations, including functional predictions of the ORFs, are provided in Supplementary Table 2.

Phage vB_AbaSI_1 harbors a total of 75 genes, with 45 (60.0%) classified as hypothetical proteins of unknown function, underscoring the limited functional characterization of many phage genes. The remaining 30 genes (40.0%) have identifiable functions and are organized into seven functional modules: (i) packaging module, (ii) capsid module, (iii) tail module, (iv) lysis module, (v) DNA replication and repair module, (vi) lysogeny module, and (vii) miscellaneous module (Fig. 2). The packaging module is comprised of a single gene encoding the terminase large subunit, a critical enzyme responsible for packaging viral DNA into the capsid during assembly. In the capsid module, genes encoding minor and major capsid proteins were identified, which are essential for the structural integrity and assembly of the phage particle. The tail module contains seven genes, including the tape measure protein. The lysis module consists of three genes: metallopeptidase, C40 family peptidase, and N-acetylmuramidase (a type of endolysin), all of which play key roles in the degradation of the bacterial cell wall, allowing for the release of progeny phages[32].

The DNA replication and repair module of phage vB_AbaSI_1 consists of seven genes, responsible for ensuring efficient replication and maintenance of the phage genome during the infection cycle. This module likely includes genes for DNA polymerases, helicases, and other enzymes that support the replication and repair of phage DNA within the host, which is essential for the viral life cycle.

Remarkably, the lysogeny module comprised of five genes, including two site-specific integrase genes, which are indicative the capacity of the phage to undergo lysogenic infection. This lysogenic characteristic suggests that phage vB_AbaSI_1 can persist within *A. baumannii* hosts without immediately causing lysis, thereby contributing to its long-term survival and potential influence on bacterial evolution. The lysogenic nature of phage vB_AbaSI_1 makes it unsuitable for direct therapeutic use but amenable to engineering for clinical applications as shown in other representation[33]. Additionally, it serves as a model for studying phage-curcumin interactions in antibacterial activity.

The miscellaneous module of phage vB_AbaSI_1 encodes four genes with diverse functions: glutamate 5-kinase (G5K), a stress-responsive nuclear envelope protein, an SOS response-associated peptidase family

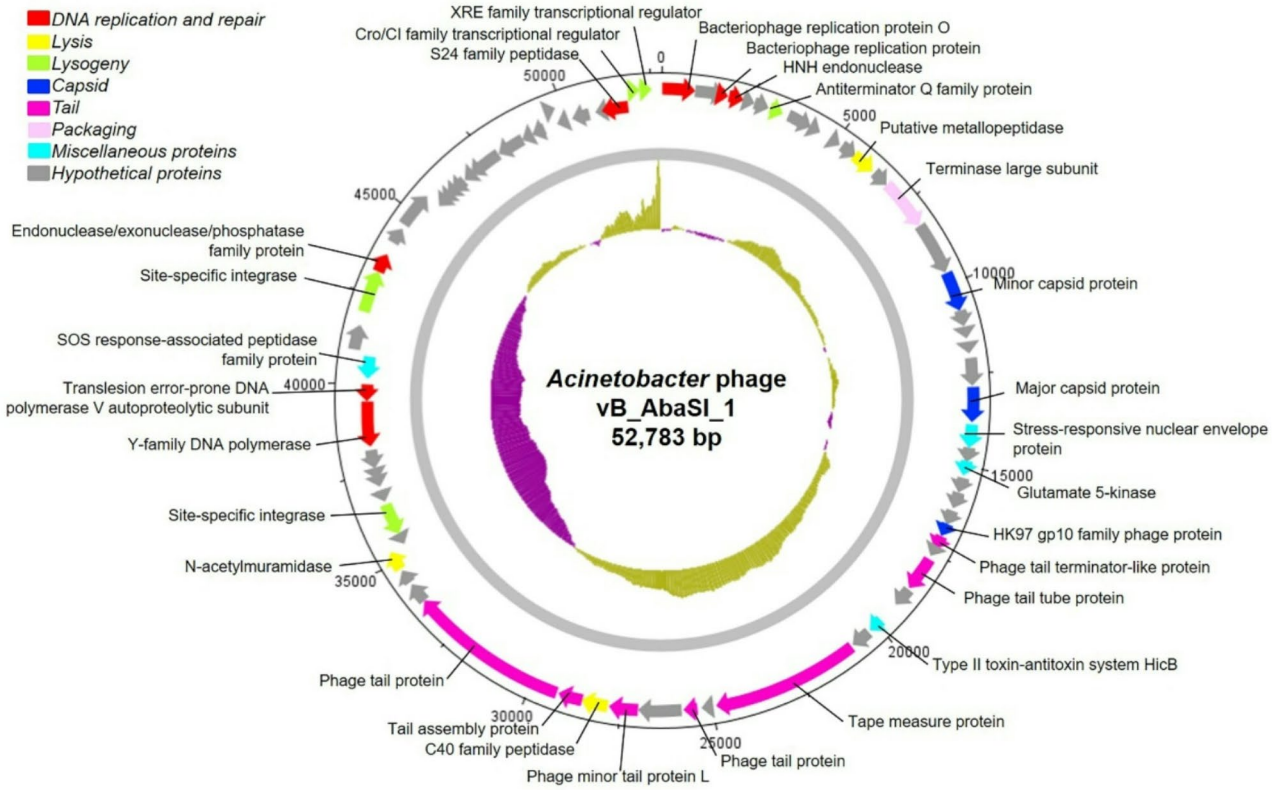

Fig. 2. Genomic map of *A. buamannii* phage vB_AbaSI_1. Phage genome visualization is shown by the dark gray circle with the unit in kilobases (kb). The circular genome map of phage vB_AbaSI_1 is organized into several functional modules, including DNA replication and repair (red), lysis (yellow), lysogeny (green), capsid (blue), tail (pink), packaging (light pink), miscellaneous proteins (cyan), and hypothetical proteins (gray). The outermost circle shows the scale in bp, with 0 representing the origin of replication. The innermost circle represents the value of the GC skew: yellow for positive and purple for negative.

protein, and a toxin-antitoxin system gene. The presence of G5K suggests a role in amino acid metabolism[34]. The stress-responsive nuclear envelope protein and SOS response-associated peptidase likely play roles in the phage's ability to cope with host-induced stress, particularly under conditions of DNA damage[35]. The toxin-antitoxin system gene is of particular interest, as such systems are often associated with bacterial stress responses and could also play a role in stabilizing the prophage within the host genome during lysogeny, preventing the host from eliminating the integrated phage DNA[36].

Overall, the presence of these modules highlights the complex interaction between phage vB_AbaSI_1 and its host. The tendency to lysogenize, combined with the presence of stress-response and replication/repair genes, suggests that vB_AbaSI_1 is well-equipped to persist in diverse environments.

Comparative genomic analysis of phage vB_AbaSI_1: identification as a novel phage species

Comparative genomic analysis revealed that phage vB_AbaSI_1 displayed close amino acid sequence similarity to *Acinetobacter* phages YMC11/11/R3177 (NC_041866.1) and YMC/09/02/B1251_ABA_BP (NC_019541.1), both of which were isolated from hospital wastewater in South Korea (Fig. 3A). In addition, nucleotide sequence comparisons revealed that phage vB_AbaSI_1 share 87.36%, 88.70%, and 89.08% average nucleotide identity (ANI) with phages YMC11/11/R3177, YMC/09/02/B1251_ABA_ BP, and AM106 (MH115576.1), respectively. As the ANI percentages are below the 95% threshold for species delineation, phage vB_AbaSI_1 qualifies as a novel phage species according to current classification standards[37].

To further confirm that phage vB_AbaSI_1 is distinct from these previously reported phages, a detailed genomic comparison was conducted between phage vB_AbaSI_1 and the three closely related phages. As shown in Fig. 3B, while phage vB_AbaSI_1 shares significant similarities in genes related to phage structure such as the packaging, capsid, tail, and lysis modules, there are notable differences in other essential genes. The structural gene conservation suggests that the basic assembly and infection mechanisms are shared across this group of phages, but the variations in replication and lysogeny-related genes may influence their behavior in different bacterial hosts. Specifically, genes in the DNA replication/repair and lysogeny modules showed significant divergence, setting phage vB_AbaSI_1 apart from other phages which may lead to its unique host interaction and survival mechanisms.

Besides genomic comparison with other phages, the relationship between phage vB_AbaSI_1 and its bacterial hosts was investigated. Homology search against the 979 *A. baumannii* genomes available in the GenBank

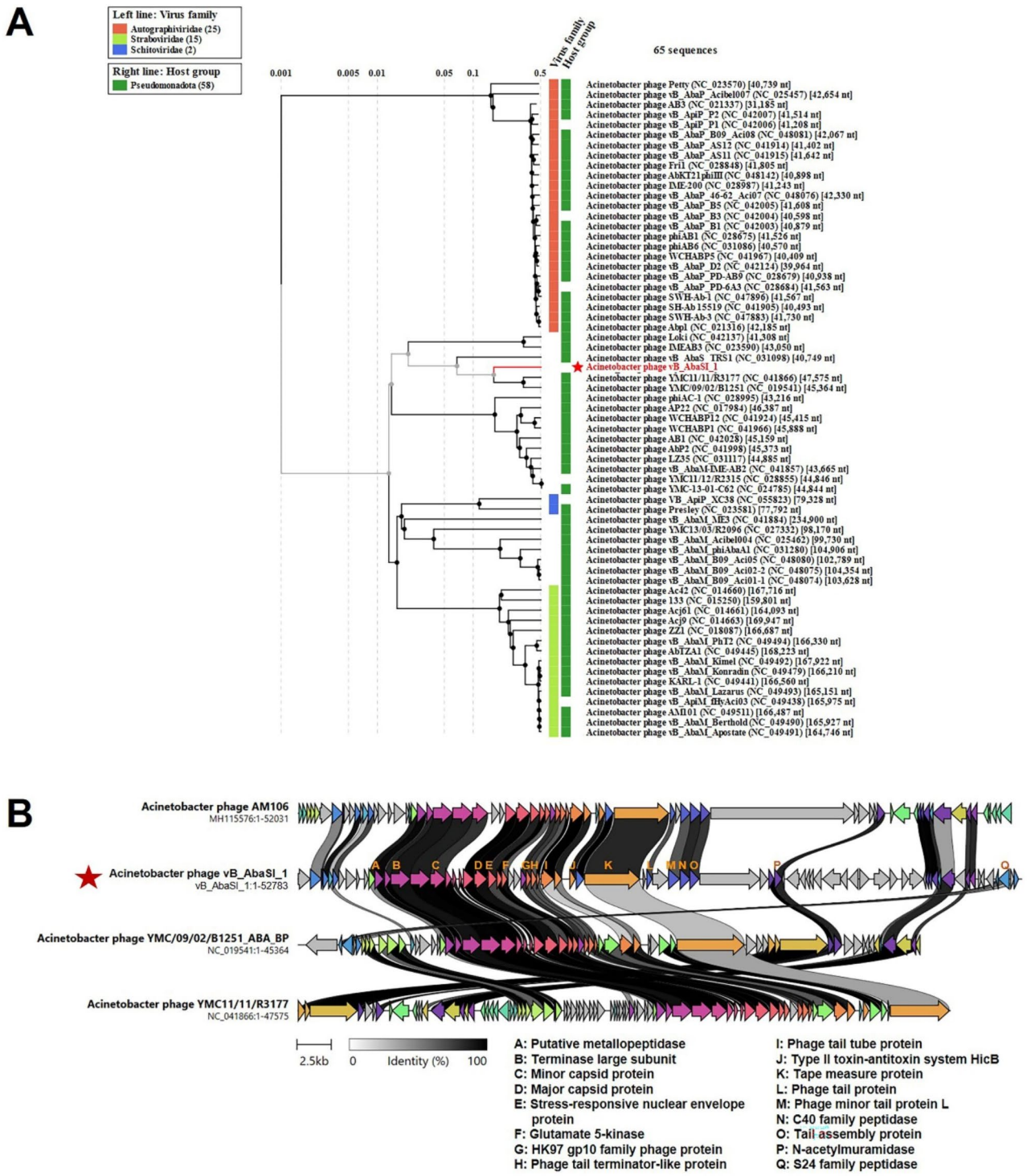

Fig. 3. Comparative genome analysis of phage vB_AbaSI_1 to other *A. baumannii* phages. (**A**) Phylogenetic tree of *Acinetobacter* phages based on nucleotide sequences. Phage vB_AbaSI_1 (marked with a red star) clusters with 65 closely related *Acinetobacter* phages, including AM106, YMC/09/02/B1251_ABA_BP, and YMC11/11/R3177. The left-hand side of the tree categorizes phages by viral family, and the right-hand side groups them by their bacterial host. (**B**) Genomic comparison of phage vB_AbaSI_1 with related *Acinetobacter* phages AM106, YMC/09/02/B1251_ABA_BP, and YMC11/11/R3177. Gene synteny and conservation are depicted, showing shared genes involved in phage structure and function. Conserved regions include genes encoding putative metallopeptidase (A), terminase large subunit (B), major capsid protein (C), tail proteins (L, M, and N), and additional phage structural components. Identical regions between genomes are shaded, indicating high sequence identity (100%), while divergent areas represent unique adaptations within the phages.

database (taxid: 470), limited to a maximum of 5,000 target sequences, revealed that only 16 out of 979 complete *A. baumannii* genomes (1.63%) carried the full phage vB_AbaSI_1 sequence suggesting that complete genome of prophage vB_AbaSI_1 is not commonly present in *A. baumannii*. Notably, all 16 isolates were derived from animal clinical samples collected in France (Supplementary Table 4).

Antibacterial efficiency of phage vB_AbaSI_1 on *A. baumannii*

To evaluate the antibacterial efficiency of phage vB_AbaSI_1, the MDR *A. baumannii* strain 131 (10^6 CFU/mL) was treated with varying concentrations of the phage: 10^5, 10^6, 10^7 and 10^8 PFU/mL, corresponding to MOIs of 0.1, 1, 10, and 100, respectively. Following incubation at 37 °C, a significant reduction in bacterial counts was observed within the first hour, indicating rapid phage activity (Fig. 4A). However, by 24 h, the bacterial population rebounded to levels similar to the untreated control group, even at the highest MOI of 100. This rebound suggests that while phage vB_AbaSI_1 is capable of an initial lysis and reduction in bacterial load, it

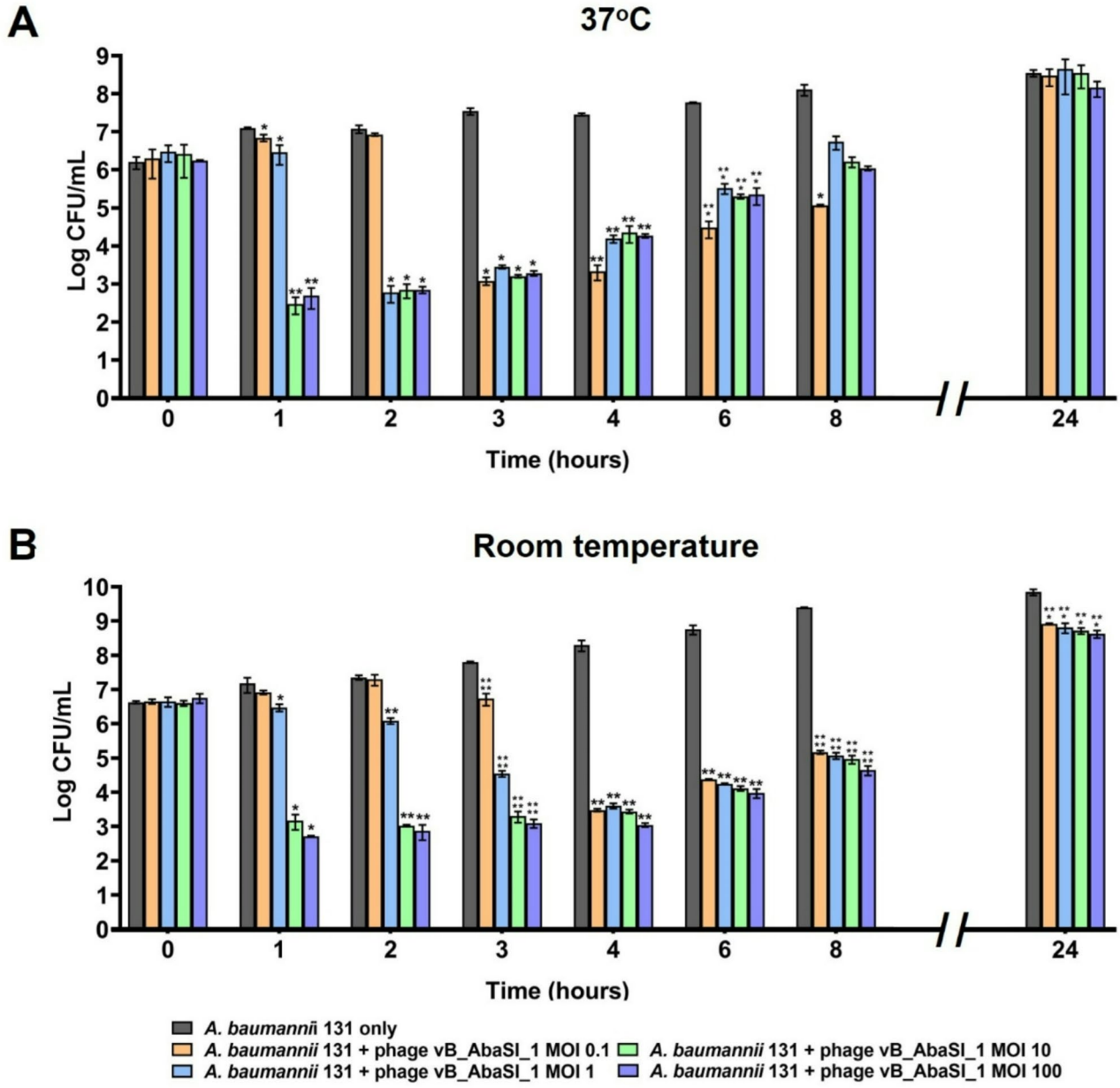

Fig. 4. Antibacterial efficiency of phage vB_AbaSI_1 against *A. baumannii*. *A. baumannii* strain 131 (10^6 CFU/mL) was treated with different MOIs (0.1, 1, 10, 100) of phage vB_AbaSI_1 at (**A**) 37 °C and (**B**) room temperature. At the indicated time points, bacterial counts (log CFU/mL) were measured. Statistical significance was considered when the *p*-value was less than 0.05 (* $P<0.05$, ** $P<0.01$, *** $P<0.001$, **** $P<0.0001$), in comparison with the untreated bacterial control at each time-point. Undetectable (UD) indicates the bacterial counts fell below detectable levels (1 CFU/mL).

is however, unable to completely eradicate the bacteria due to phage-resistance development. This allowed the bacterial population to recover over time as shown in other phage studies[38]. In addition to being a temperate phage, these findings suggest a limitation in using wild-type phage vB_AbaSI_1 without genetic modification for sustained bacterial suppression.

In addition to 37 °C, the antibacterial efficiency of phage vB_AbaSI_1 at room temperature displayed a similar ability, being able to rapidly reduce the bacterial count within 1 h (Fig. 4B). However, as with the results at 37 °C, the bacterial population eventually rebounded to control levels after 24 h, regardless of the initial phage concentration. The 24 h rebound suggests that vB_AbaSI_1 alone is insufficient for long-term control. This underscores the need for phage cocktails or combination therapies, such as with curcumin, for optimal therapeutic efficacy and to suppress phage-resistant populations.

Exploration of antibacterial activity of curcumin with phage vB_AbaSI_1

Antibacterial properties of curcumin against *A. baumannii* were evaluated by testing against cultures of ten representative *A. baumannii* isolates: six antibiotic-resistant isolates (131, E4, 036, B1, B8, and D6) and four antibiotic-susceptible isolates (91018, 90855, 1084, and 510). After 24 h incubation at 37 °C with curcumin, only *A. baumannii* isolate 131 exhibited a statistically significant reduction in bacterial counts. The remaining nine isolates (90%), showed no significant bacterial reduction compared to the untreated control group (Fig. S2A). These findings indicate that, under the tested conditions, curcumin alone was largely ineffective at reducing the bacterial load not only the drug-resistant, but also drug-susceptible *A. baumannii* isolates.

Subsequently, the effect of curcumin on the viability of phage vB_AbaSI_1 was investigated. The results demonstrated that the reductions in phage viability at 100, 200, and 400 µg/mL were not significantly different from each other. In contrast, a statistically significant reduction in phage viability occurred at the highest concentration of 600 µg/mL (Fig. S2B). Based on these findings, the 400 µg/mL concentration of curcumin was selected for subsequent combination experiments with phage vB_AbaSI_1.

Combining curcumin and phage vB_AbaSI_1 enhanced antibacterial activity

Next, phage vB_AbaSI_1 and curcumin were combined and investigated to ascertain if the observed antibacterial activity could be enhanced. As shown in Fig. 5, no viable MDR-*A. baumannii* 131 were detected 1-h post-treatment (T1) when treated with curcumin and phages simultaneously at two different MOIs (10 and 100). Similarly, at 3-h post-treatment (T3), no viable MDR-*A. baumannii* 131 were detected and the effect was observed not only at MOIs 10 and 100 but also extended to MOIs 1.0 and 0.1 (Fig. 5). In contrast, when curcumin or phage were administered individually, bacteria growth was observed. This indicates that combining curcumin with the phage exerted a synergistic efficacy against MDR-*A. baumannii* 131, outperforming the effect of either individual treatment.

Next, the antibacterial efficiency of the treatments was extended up to 24 h. As shown in Fig. 6, treatment with phage and curcumin combination (orange bars) could eliminate *A. baumannii* 131, with no detectable bacteria from 1 to 3 h. No significant difference in the killing efficiencies of the three different phage vB_AbaSI_1 concentrations (MOIs 10, 50 and 100) with the extract. In contrast, when only curcumin (Fig. 6A-C, yellow bars) or only phage (Fig. 6A-C, green bars) were used, the bacterial count was reduced to undetectable levels only for 1 h, but then rebounded between 2 and 8 h, surpassing the results seen with all phage and curcumin combinations. This data further supports our earlier observation that the combination of curcumin and phage

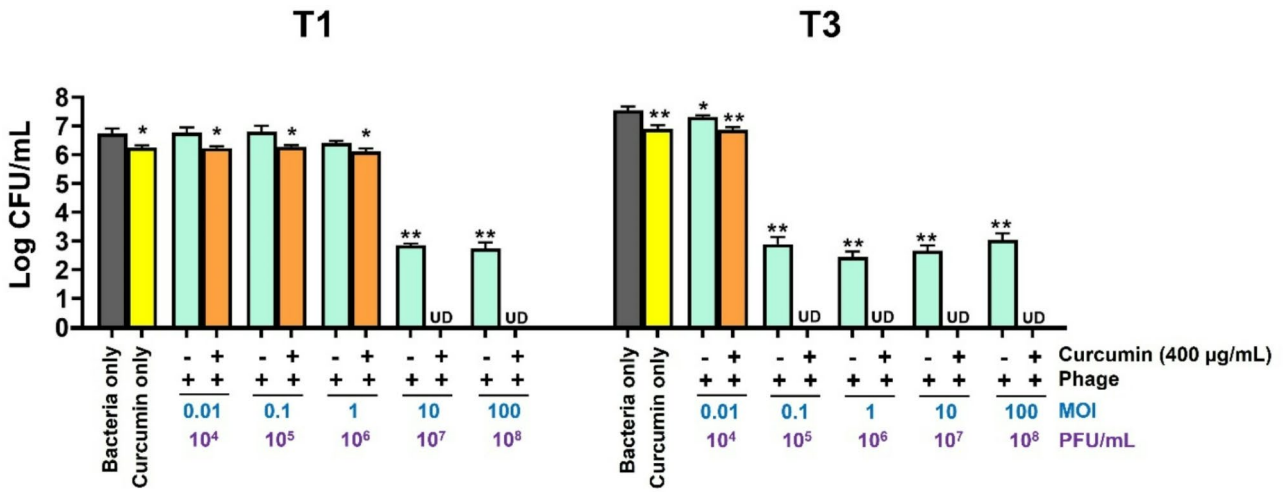

Fig. 5. Combined antibacterial effect of phage vB_AbaSI_1 and curcumin against *A. baumannii*. The number of *A. baumannii* isolate 131 at T1 (1 h) and T3 (3 h) after treatment with curcumin (400 µg/mL) and varying concentrations of phage vB_AbaSI_1 (MOI 0.01–100; 10^4–10^8 PFU/mL). Statistical significance was considered when the *p*-value was less than 0.05 (* $P < 0.05$, ** $P < 0.01$), in comparison with the untreated bacterial control at each time-point. Undetectable (UD) indicates the bacterial counts fell below detectable levels (1 CFU/mL).

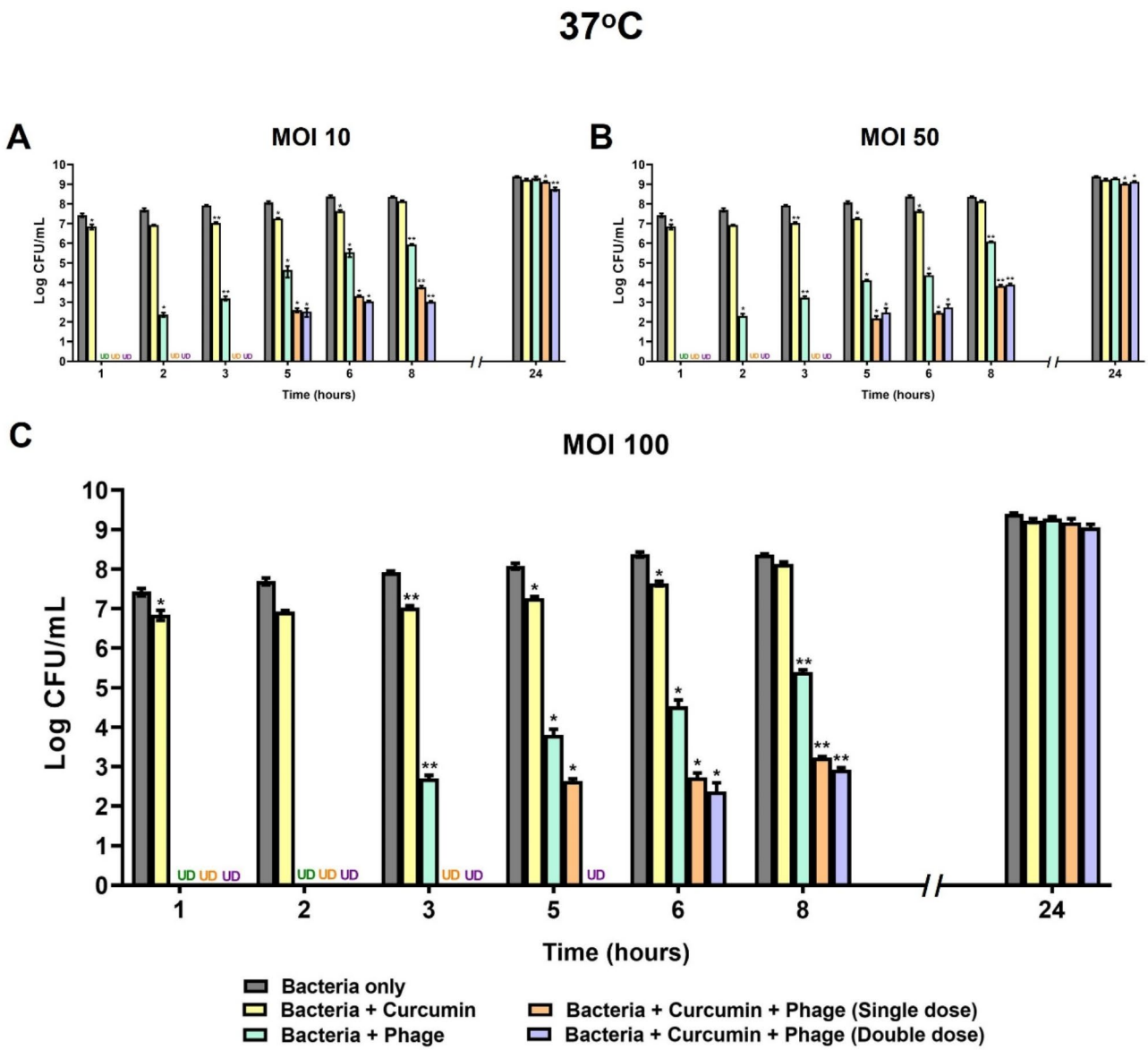

Fig. 6. The antibacterial activity of curcumin and phage vB_AbaSI_1 combination at 37 °C. Time-kill assay at MOIs 10 (**A**), 50 (**B**), and 100 (**C**). The number of *A. baumannii* isolate 131 were measured over 24 h for *A. baumannii* treated with curcumin (400 µg/mL) alone, phage vB_AbaSI_1 alone (1×10^7, 0.5×10^8, 1×10^8 PFU/mL), and a combination of curcumin/phage with either single or double doses. Statistical significance was considered when the *p*-value was less than 0.05 (* $P<0.05$, ** $P<0.01$), in comparison with the untreated bacterial control at each time-point. Undetectable (UD) indicates the bacterial counts fell below detectable levels (1 CFU/mL).

produced a synergistic effect, controlling bacterial growth more effectively than either bio-active component alone. However, at 24 h post-treatment, the bacterial count rebounded to levels equivalent to the untreated control (Fig. 6A-C).

To prolong the antibacterial efficacy of the combination treatment beyond 3 h, a second dose of the phage vB_AbaSI_1/curcumin combination at 1 h was administered in addition to the initial dose. The results showed that among 3 different MOIs of the phage with curcumin combination, only the combination with MOI 100, could extend the period of bacterial reduction to undetectable levels from 3 to 5 h (Fig. 6C, purple bars). In contrast, the lower MOIs (10, and 50) of phage added in the combination treatment did not extend period of undetectable bacteria, with only suppression of bacterial growth for 3 h was seen (Fig. 6B-C, purple bars). Notably, the bacterial counts rebounded to levels equivalent to the untreated control at 24 h post-treatment. Here, combining curcumin (400 µg/mL) with phage vB_AbaSI_1 (10^8 PFU/mL) could eliminate *A. baumannii* 131, with no detectable bacteria up to 3 h and up to 5 h when having double dose treatment.

Temperature affects the synergistic efficacy of combination treatment

Besides efficacy at 37 °C, the antibacterial activity of the curcumin and phage vB_AbaSI_1 combinations were also tested at room temperature (25 °C). Figure 7A-C (orange bars), showed that no bacterial growth was detected for all three different MOIs for the combined curcumin/phage single dose treatment. The enhancement was observed in double dose treatment (administered at 0 and 1 h), the period of undetectable bacteria was extended from 5 to 6 h for all three conditions (Fig. 7A-C, purple bars).

At the 24 h mark, although *A. baumannii* was still detectable, the bacterial counts following treatment with all combinations at room temperature were significantly lower, with a reduction of 3 logs, compared to the untreated control (Fig. 7A-C, purple bars compared to the grey bars). This indicates that the curcumin and phage combinations were more effective at reducing bacterial counts at room temperature than at 37 °C. This finding may have an advantage for the treatment of surface infection where the temperature may be lower than 37 °C.

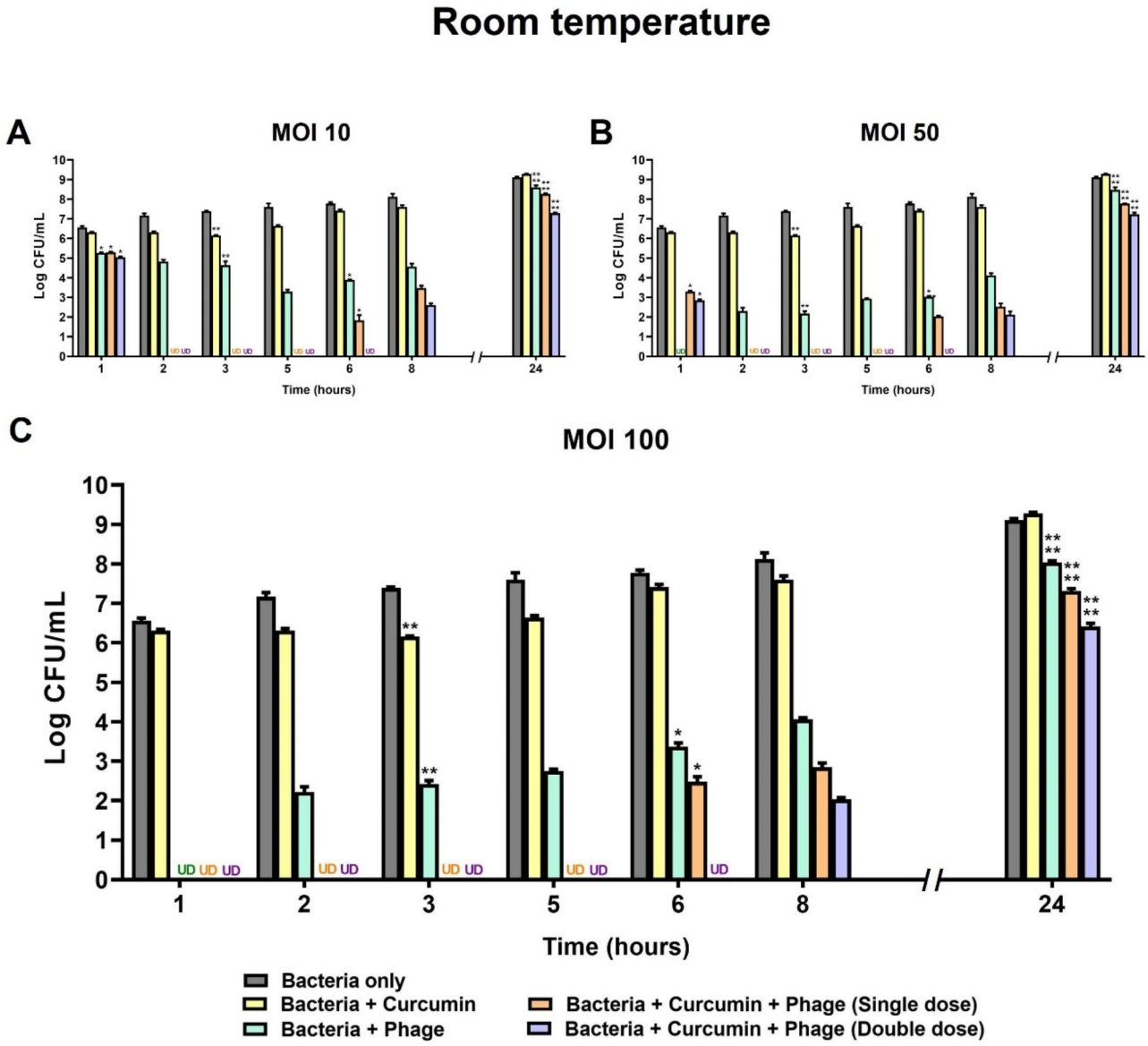

Fig. 7. The antibacterial activity of curcumin and phage vB_AbaSI_1 combination at room temperature. Time-kill assay at MOIs 10 (**A**), 50 (**B**), and 100 (**C**). The number of *A. baumannii* isolate 131were measured over 24 h for *A. baumannii* treated with curcumin (400 µg/mL) alone, phage vB_AbaSI_1 alone (1×10^7, 0.5×10^8, 1×10^8 PFU/mL), and a combination of curcumin/phage with either single or double doses. Statistical significance was considered when the *p*-value was less than 0.05 (* $P < 0.05$, ** $P < 0.01$, **** $P < 0.0001$), in comparison with the untreated bacterial control at each time-point. Undetectable (UD) indicates the bacterial counts fell below detectable levels (1 CFU/mL).

Phage infection as a key determinant of antibacterial synergistic effects

To explore the synergistic mechanism of curcumin/phage combination as an antibacterial agent against *A. baumannii*, two groups of *A. baumannii* isolates including (1) vB_AbaSI_1-susceptible *A. baumannii* strains (131 and DMST43250) and (2) vB_AbaSI_1-resistant *A. baumannii* strains (90855 and PB571) were treated with either phage vB_AbaSI_1 or curcumin alone or combined curcumin/phage. The results showed that the bacterial counts of *A. baumannii* strain 131 (Fig. 8A) and DMST43250 (Fig. 8B) decreased more significantly than with either phage or curcumin alone, at both 3–5 h post-treatment indicating a synergistic effect in bacterial killing with the phage vB_AbaSI_1-susceptible *A. baumannii* strains. On the contrary, no synergistic effect was observed in the *A. baumannii* isolates 90855 (Fig. 8C) and PB571 (Fig. 8D) which could not be infected by phage vB_AbaSI_1 (vB_AbaSI_1-resistant *A. baumannii* strains) suggesting that the synergistic mechanism of curcumin and phage relies heavily on the ability of the phage vB_AbaSI_1 to interact with or infect the bacteria. The possible mechanism may be due to the initial phage infection which promote the penetration of curcumin through the peptidoglycan in the bacterial cell wall, thereby enhancing bacterial killing.

Discussion

Phages are viruses which specifically infect bacteria and they are recognized as the earth's most abundant biological entities. Not all of the isolated phages are suitable for phage therapy, the suitable ones should be strictly virulent (also known as lytic phages) that can only access a lytic life cycle. Though not ideal, previous therapeutic studies have explored temperate phages where strictly lytic ones are not found to provide foundation to improve their deployment in clinical application[33]. Temperate phages are found freely in the environment but can integrate into bacterial chromosome[39]. To examine the prophage content of our test host, the MMC induction assay was employed. This is to enable the identification of a suitable *A. baumannii* isolate for phage isolation. This study revealed that a large proportion of *A. baumannii* isolates (~93%) from Thailand harbored MMC-inducible prophages, consistent with previous reports indicating that prophages are a common feature in *A. baumannii* genomes[40]. The incidence observed was significantly higher than the in silico analyses, which estimate prophages in only ~ 46% of bacterial genomes[41].

The isolated phage vB_AbaSI_1 has properties that promote its antibacterial activity including the formation of distinct halo plaques on *A. baumannii* strain 131, indicating the presence of depolymerase enzymes that can degrade bacterial capsule polysaccharides (CPS) and exopolysaccharides (EPS), which are essential components of bacterial biofilms and protective barriers[42]. The ability of phages to produce such enzymes is crucial for efficient bacterial lysis and have been observed in other *A. baumannii* phages, such as phages vB_AbaM_B9, AM24, and p54[43–45]. Another factor that promotes its potential application in phage therapy is its ability to remain active at 37 °C, the normal human body temperature, along with its pH stability in acidic and alkaline conditions (pH 3-7) and (up to pH 11), respectively, favored its suitability for clinical application. Additionally, phage vB_AbaSI_1 exhibited a short latent period of 30 min and a large burst size of 136 PFU/cell, making it highly efficient in lysing bacterial cells quickly. This is comparable to other *A. baumannii* phages, such as Abp9, which has a similar latent period but a slightly larger burst size[46].

Despite its efficiency, phage vB_AbaSI_1 had a relatively narrow host range, lysing only 23.8% of the *A. baumannii* strains tested. Other *A. baumannii* phages that were found to have a very narrow host range (less than 30%) such as ϕAB1–9 and ϕAB11[47]. However, phage like EAb13 has a broader host range, lysing up to 86.7% of diverse drug-resistant *A. baumannii* isolates[48]. The narrow host range of phage vB_AbaSI_1 may be attributed to the presence of a vB_AbaSI_1-like prophage in the bacterial host genome, potentially triggering superinfection exclusion, which blocks infection by closely related phages[49]. Moreover, a narrow host range can also result from phage resistance evolving rapidly, especially in high-burden infections with potentially higher resistant populations[50]. This evolution can limit the long-term efficacy of single-phage monotherapy. To address this, phage cocktails targeting multiple bacterial receptors with complementary targets can enhance infection treatment success[51]. Another strategy is phage engineering, where receptor-binding proteins are modified to broaden host range[52].

The presence of integrase genes limits the therapeutic potential of phage vB_AbaSI_1 for therapeutic application. To overcome the problem, phage engineering to delete integrase will make it therapeutically acceptable. For instance, a 15-year-old cystic fibrosis patient with disseminated *Mycobacterium abscessus* infection experienced significant clinical improvement following treatment with a three-phage cocktail that was developed through engineering to remove phage repressor gene[33]. The other possible approach to overcome the lysogenic property is the use of phage-derived enzymes, such as depolymerases, which have potent bactericidal activity by degrading bacterial cell walls and biofilms[53]. Hence, instead of using whole temperate phage vB_AbaSI_1, recombinant depolymerases could be combined with curcumin to avoid limitation of temperate phage application, enhance bacterial killing and minimizing the risk of bacterial resistance.

Previous studies have shown that curcumin can act synergistically with antibiotics to enhance bacterial killing, especially against drug-resistant strains[28,54]. In this study, combination of phage vB_AbaSI_1 and curcumin exhibited significant synergistic antibacterial effects against *A. baumannii* strain 131. Complete bacterial elimination was achieved within 1 h of treatment at 37 °C, and an extended bacteria-free period of up to 5 h was observed following a double dose of both phage and curcumin, administered at 0 and 1 h. The similar protocol treatment at room temperature further extended the bacteria-free period up to 6 h. This study highlighted the synergy of curcumin/phage combination in inhibiting bacterial growth.

The possible mechanism of synergistic effect may result from phage vB_AbaSI_1 facilitating curcumin penetration into bacterial cells by degrading the bacterial cell wall. This is supported by the observed lack of synergistic effects in phage-resistant strains, such as *A. baumannii* strains 90855 and PB571, where the phage was unable to infect the bacteria and therefore could not enhance curcumin's efficacy. When phages penetrate bacterial cell wall, they may facilitate curcumin entry into the cytoplasm, triggering a cascade of antibacterial

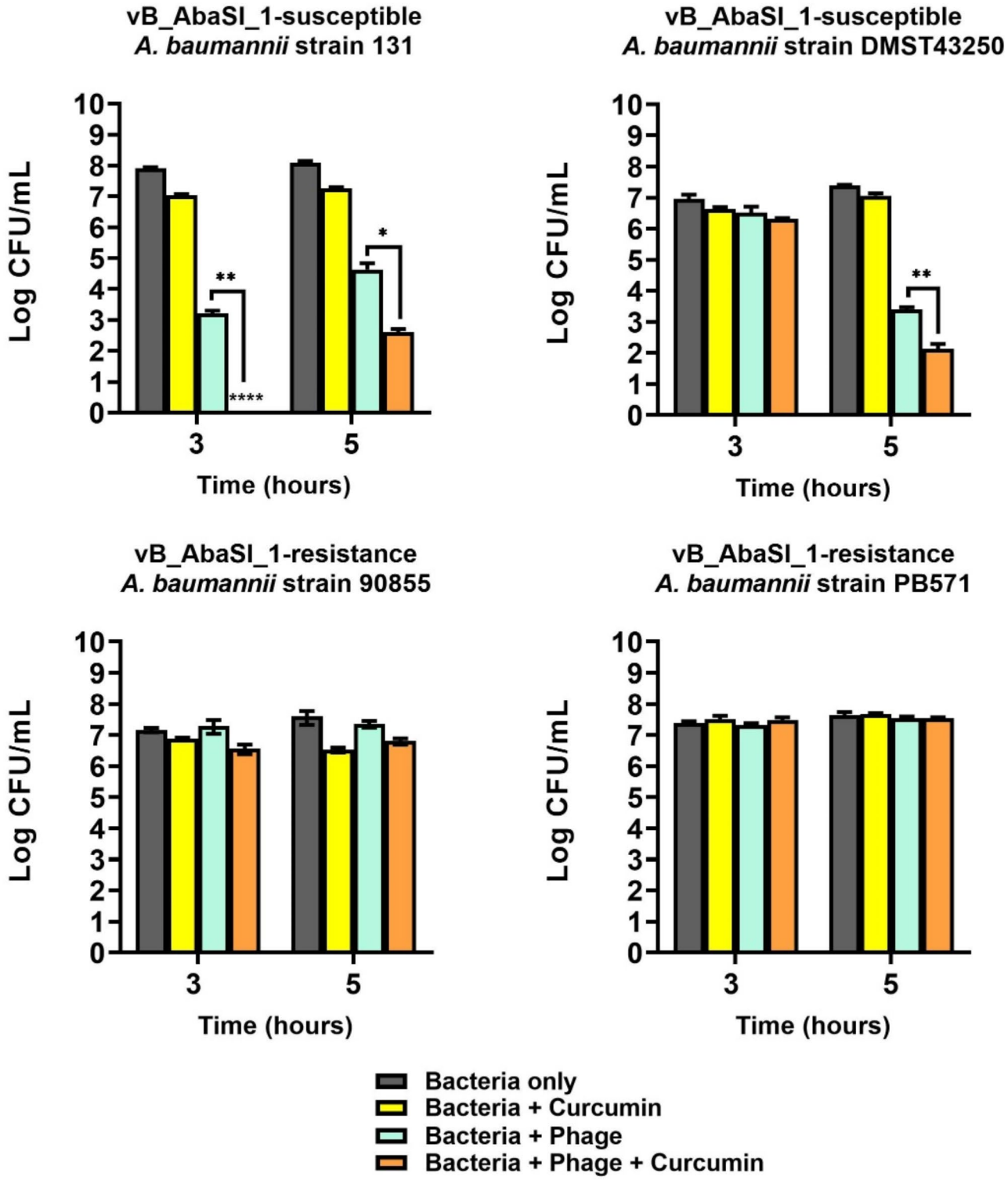

Fig. 8. Comparison of phage/curcumin combination treatment between phage-susceptible and phage-resistant *A. baumannii* strains. Phage vB_AbaSI_1-susceptible *A. baumannii* strains 131 (**A**) and DMST43250 (**B**), were compared with phage vB_AbaSI_1-resistant *A. baumannii* strains 90855 (**C**) and PB571 (**D**) following treatment with either phage vB_AbaSI_1 alone (MOI 100), curcumin alone (400 µg/mL), or a combination of both. Viable bacterial counts were measured by colony count with untreated bacteria serving as controls. Data are presented as mean ± standard deviation (SD) from three independent experiments conducted in triplicate. Statistical significance was considered when the *p*-value was less than 0.05 (* $P < 0.05$, ** $P < 0.01$, **** $P < 0.0001$).

actions. Once inside, curcumin disrupts the bacterial membrane by embedding in the lipid bilayer, leading to increased permeability, ion leakage, membrane potential loss, and structural damage[55]. Simultaneously, curcumin was reported to inhibit bacterial cell division by binding to the GTP-binding site of the FtsZ protein, preventing its polymerization into the Z-ring structure[56]. Not only structural interference, but curcumin had also been shown to inhibit quorum sensing, a bacterial communication system, reducing biofilm formation and virulence factor production as demonstrated in *P. aeruginosa*[57]. In *Salmonella*, curcumin was reported to downregulate the activity of SPI1 genes involved in *Salmonella* entry into epithelial cells suggesting its involvement in bacterial pathogenesis[58].

Furthermore, curcumin can generate reactive oxygen species, causing bacterial cellular damage and apoptosis[59]. Additionally, curcumin may also disrupt bacterial metabolic enzymes, such as dipeptidyl peptidases (DPPs), leading to the inhibition of nucleic acid synthesis and key metabolic pathways, as demonstrated in *Porphyromonas gingivalis*[60]. These mechanisms, which target multiple essential bacterial processes simultaneously, promote curcumin a potent antibacterial agent in disrupting bacterial functions and combating infections.

A. baumannii is known for its ability to colonize burn wounds, often leading to systemic infections[61], making wound treatment extremely difficult. According to the data here, development of an antimicrobial skin gel or emulsion from the combination of phage vB_AbaSI_1 or the phage lytic enzymes and curcumin will be an attractive alternative treatment for *A. baumannii*-infected skin. Including curcumin in the combination will not only provide antibacterial properties but also provides additional benefits of reducing the inflammatory response in wounds due to the curcumin's anti-inflammatory activity[27]. This idea was supported by previous study that curcumin-loaded myristic acid microemulsion with curcumin could inhibited 50% of the *Staphylococcus epidermidis* growth on the skin[62].

The possible explanations for the regrowth of *A. baumannii* after 24 h treatment with curcumin-phage vB_AbaSI_1 combination may arise from several reasons. Firstly, through mutations in bacterial surface receptors for phage infection or anti-phage defense systems[63]. Secondly, the unstable nature of curcumin in biological environments may limit its long-term efficacy. Curcumin is prone to degradation under physiological conditions, which could reduce its antibacterial activity over time[28]. Thus, requiring formulation either alone or with the phage to enhance optimal stability and delivery. Third, phage vB_AbaSI_1 is a temperate phage, meaning it can integrate into the bacterial genome and enter a lysogenic cycle, which might limit its bactericidal activity compared to strictly lytic phages. Lastly, at 24 h post-treatment, *A. baumannii* may generate biofilm that can protect bacteria from both phage infection and curcumin penetration. Investigation of these possible causes of this phenomenon warren further study.

In conclusion, using phage vB_AbaSI_1 as a model, the combination of curcumin with phage generates a synergistic antibacterial activity effectively reducing bacterial counts to undetectable levels up to 5 h and 6 h at 37 °C and room temperature, respectively. Although after 24 h, the bacteria rebounded to the same level as the control at 37 °C, 3 logs reduction was observed at room temperature. Moreover, the study revealed that the mechanism of synergy depends on the ability of the phage to infect the bacteria. Future studies should emphasize the use of phage-derived enzymes rather than the whole phage engineering the phage to make it therapeutically acceptable, and optimizing the combination, dosing, and delivery methods for wound-infected MDR *A. baumannii*.

Materials and methods

Biosafety approval

This research project was approved by the Institutional Biosafety Committee-IBC, Faculty of Medicine Siriraj Hospital, Mahidol University. The approval certificate numbers are SI 2021-006 and SI 2023-028.

Bacterial strains and culture condition

All bacterial isolates used in this study are listed in Table 1. They were cultured in Luria-Bertani (LB) broth (Criterion™, Hardy Diagnostics, USA) at 37 °C with shaking for 18–24 h. Mid-log phase *A. baumannii* was obtained by subculturing 100 µL of overnight culture into 10 mL of fresh LB broth and incubating at 37 °C for 4 h until OD600 ~ 0.17–0.2 (~ 10^8 CFU/mL).

Curcumin Preparation

Curcumin (MedChemExpress, USA) extracted from *Curcuma longa* (CAS No. 458-37-7) was dissolved in 1 mL 100% dimethyl sulfoxide (DMSO) to the concentration of 20 mg/mL. After preparation, the curcumin suspension was stored in a dark place at a temperature of 2–8 °C and used within 4 weeks. For testing the antibacterial activity, the final concentration is 400 µg/mL in the culture medium.

Mitomycin-C induction assay

The MMC-induction assay was performed according to Lucidi et al.[64]. Essentially, mid-log phase *A. baumannii* cultures (~ 10^8 CFU/mL) were treated to a final concentration of 1 µg/mL of MMC (Sigma-Aldrich, Missouri, USA) and further incubated at 37 °C for 4–6 h. Afterwards, the cultures were centrifuged, and the supernatants were filtered through a 0.45 µm filter (GE Healthcare Life Sciences, Marlborough, USA). The filtrates were then analyzed for the release of infecting prophages using a spot assay against a panel of *A. baumannii* strains (Supplementary Table 1). Presence of infecting phages as indicated by the production of clear plaques signify the potential presence of MMC-inducible prophages within the *A. baumannii* genome. This is a screening assay to identify the suitable host strains for phage isolation. However, this assay cannot rule out the possibility that some bacteria may contain prophages that could not be induced by MMC or the induced prophages could not infect the bacterial host.

Sewage collection and phage isolation assay

A total of 100 sewage samples were collected from multiple provinces in the central part of Thailand, including Bangkok, Pathum Thani, Ayutthaya, Ang Thong, Nonthaburi, and Sing Buri provinces, between May 2021 and August 2023. Samples were collected in sterile bottles and filtered through a 0.45 µm filter (Whatman™, UK). Each filtrate (approximately 100 mL) was mixed with an equal volume of double concentrate (2X) LB broth (Criterion™, Hardy Diagnostics, USA) and 500 µL of *A. baumannii* strain 131 (~ 10^8 CFU/mL) for phage enrichment. The mixtures were incubated at 37 °C for 48 h followed by centrifugation and filtration as described above. The filtrates were subjected to phage isolation using spot test as described below. Individual clear plaques were selected and purified through at least ten rounds of double agar overlay plaque assays, also described below. For phage propagation, the double agar overlay plaque assay was conducted using approximately 30 petri dishes per sample according to previous published paper[65].

Spot test

The spot test is a phage screening technique to identify a range of bacterial isolates phages present can lyse[65]. Confluent culture of *A. baumannii* was prepared with 100 µL volume of mid-log phase bacterial culture (10^8 CFU/mL) mixed with 5 mL of LB broth (Criterion™, Hardy Diagnostics, USA) containing 0.35% w/v agar (Titan Biotech Ltd, India) (sustained at ~ 55 ºC). The mixture of mid-log bacterial culture and LB top agar was poured onto LB 1% w/v (agar) plates and allowed to set for ~ 5 min at ambient conditions. Afterwards, 10 µL aliquots of filtered sample to be tested for phages were applied onto the surface of the prepared bacterial confluent culture and incubated at 37 °C for 16–18 h. The presence of lysis zones afterwards indicates the possible presence of infective phages in the sample, which should be further confirmed using the double agar overlay plaque assay.

Double agar overlay plaque assay and phage propagation assay

The double agar overlay plaque assay was performed as previously described[65]. Briefly, confluent bacterial culture was prepared as above with 100 µL of the filtered sample before pouring onto LB agar plates. The plates were incubated overnight and a single clear plaque was picked using sterile pipette tip and transferred to 1 mL phage buffer (100 mM NaCl, 8 mM $MgSO_4 \cdot 7\ H_2O$, 50 mM Tris-HCl, pH 7.5). The mixture was centrifuged at 15,000×g for 15 min and the supernatant was used to repeat the plaque assay. This was repeated five time to obtain a clonal phage.

To propagate phage for further characterization, the double agar overlay plaque assay was performed on ~ 30 plates per sample. After overnight incubation, phage buffer was added to each plate and incubated at room temperature for 4 h with shaking at 80 rpm. The lysates were collected, centrifuged, and the supernatant filtered through a 0.45 µm filter membrane (Whatman™, UK) before centrifugation again at 18,000×g for 30 min at 4 °C. The phage pellet was then resuspended in phage buffer and stored at 4 °C for further analysis.

Transmission electron microscopy

The morphology of isolated phages was analysed by transmission electron microscopy after negative-staining the samples[66]. The procedure involved fixing the phages (10^8 PFU/mL) with 2.5% glutaraldehyde in 0.1 M PBS (pH 7.3), followed by staining with 1% uranyl acetate on 200 mesh Formvar-carbon-coated copper grids (Electron Microscopy Sciences, Hatfield, PA, USA). The phage morphology was captured using a JEM 1400 transmission electron microscope (JOEL Co., Japan) operating at an accelerating voltage of 80 kV. Phage dimensions were analyzed using ImageJ software (version 1.49), with measurements taken from at least 20 individual phage particles to ensure accuracy and consistency.

One-step growth curve of phage infection

The phage amplification kinetics was determined using the one-step growth curve procedure[67]. To do this, phage vB_AbaSI_1 was mixed with *A. baumannii* isolate 131 at an MOI of 0.01, followed by incubation at 37 °C for 15 min. After centrifugation, the bacterial pellet was resuspended in LB broth containing 5 mM $CaCl_2$ and incubated at 37 °C. Samples of 1 mL were collected every 5 min for a total duration of 2 h. The collected samples were serially diluted and then assessed for the number of viable phages using the double agar overlay plaque assay described above. The resulting data was used to construct the phage's one-step growth curve, which helps determine the latent, log and stationary periods, and the burst size which indicate the number of phages released from a single bacterial cell.

Phage thermal and pH stability assays

Stability of phages under different pH was determined by incubating the phages (10^8 PFU/mL) with SM buffer at pH ranging from 1, 3, 5, 7, 9, 11 and 13. For acidic conditions, HCl was used to adjust the acidic pH, while NaOH was used for alkaline pH levels. For each condition, 100 µL of phage stock (10^9 PFU/mL) was added to 900 µL of the prepared pH buffer solution (to produce a target phage titre of 10^8 PFU/mL) before being incubated for 0, 6, and 24 h to assess phage stability. For thermal stability assay, phage suspension (10^5 PFU/mL) was incubated at 4 °C, room temperature, 37–45 °C for 6, 24, and 48 h. At the indicated time points, phage viability was determined by spot assay. Remarkably, in pH stability tests, extreme pH can destabilize phages or affect their binding to bacteria, so a higher bacterial concentration is used compared to temperature stability tests.

Phage genomic DNA extraction

Genomic DNA of phage was extracted by phenol-chloroform-isoamyl alcohol (PCI) extraction protocol with some modifications[65]. In brief, purified phage suspension (10^8 PFU/mL) was mixed with 5 mM of $MgCl_2$, 1 µg/mL of DNase I, and 20 µg/mL of RNase A (Thermo Fisher Scientific, USA) before being incubated for 30 min at room temperature. After incubation, 50 µg/mL of proteinase K (Thermo Fisher Scientific, USA), 20 mM of

EDTA, and 0.5% of SDS were added into the mixture before being incubated at 55 °C for 1 h. Then, the mixture was subjected to phenol/chloroform/isoamyl alcohol extraction. After centrifugation, the top aqueous layer was collected for DNA precipitation with 95% ethanol and sodium acetate. After washing with 70% ethanol, phage genomic DNA pellet was dissolved in nuclease-free water and stored at − 20 °C.

Whole genome sequencing and analysis

The whole genome sequencing and analysis of the isolated phage was performed as previously described[65]. Essentially, the genomic DNA library of phage was prepared using the Illumina DNA Library Prep kit (Illumina, Inc., US) before sequencing using the Illumina MiSeq platform and annotating according to previous report[65]. To compare phylogenetic phage proteomes, phage genome sequences were uploaded into ViPTree[68]. Comparative genome contents were visualized and compared using Clinker v0.0.25[69]. Virulence factors and antimicrobial resistance genes encoded by the phage sequences were extracted using PhageScope[70].

Host range of phages

The host range was determined according as previously described[71]. In brief, confluent semi-solid agar cultures of each of the 131 clinically isolated and standard *A. baumannii* strains together with other Gram-negative and Gram-positive bacteria, including *K. pneumoniae*, *P. aeruginosa*, *E. coli*, *S. aureus*, and *Burkholderia thailandensis* were prepared as explained above. A 10 µL droplet of the phage lysate (10^8 PFU/mL) was applied onto the bacterial confluent culture and incubated at 37 °C. Lysis zones were classified as clear (complete clearance), turbid (partial clearance), or none (no lysis). Clear and turbid zones of lysis were confirmed by the double agar overlay plaque assay.

Antibacterial activity of phage vB_AbaSI_1 against *A. baumannii*

A. baumannii (10^7 CFU/mL) was incubated with serial dilutions of phage vB_AbaSI_1 suspension, leading to final phage concentrations of 10^5, 10^6, 10^7, and 10^8 PFU/mL, resulting in MOIs of 0.1, 1, 10, and 100, respectively. The mixtures were incubated at 37 °C or left at room temperature (~27–30 °C), and viable bacteria were enumerated at 1, 2, 3, 4, 6, 8, and 24 h on LB agar compared with the initial concentration (0 h). The control for this experiment consists of *A. baumannii* cultures treated with the same volume of LB instead of the phage.

Antibacterial activity of curcumin

Six antibiotic-resistant *A. baumannii* strains (131, E4, 036, B1, B8, D6) and 4 antibiotic-susceptible strains (91018, 90855, 1084, 510), each with concentration of 10^6 CFU/mL, were treated with 20 µL of curcumin stock suspension (20 mg/mL) to achieve a final concentration of 400 µg/mL of curcumin (MedChem Express, USA) in the cultures. A control tube was prepared, consisting of cultures of each bacterial isolate without the addition of curcumin suspension. All treated cultures were incubated at 37 °C before sampling at the same time points as above to enumerate *A. baumannii* present as described above.

Assessment of the effects of curcumin on phage viability

To determine the appropriate concentration of curcumin suspension that can be combined with phages without affecting their viability, the experiment was performed using a 96-well microtiter plate. Phages (10^5 PFU/mL) were mixed with dissolved curcumin suspension to final concentrations of 600, 400, 200, and 100 µg/mL, respectively. Control wells were treated with DMSO alone. The plates were incubated at 37 °C for 3 and 24 h. Viable phages were 10-fold serially diluted and enumerated by spot assay.

Antibacterial activity of phage and curcumin combination treatment

The cultures of *A. baumannii* isolate 131 at a concentration of 1×10^6 CFU/mL were treated with (i) phage alone at concentrations of 1×10^4, 1×10^5, 1×10^6, 1×10^7, 0.5×10^8, and 1×10^8 PFU/mL (corresponding to MOIs of 0.01, 0.1, 1, 10, 50, and 100, respectively), (ii) curcumin suspension alone at 400 µg/mL, (iii) a single dose of both phage (1×10^4, 1×10^5, 1×10^6, 1×10^7, 0.5×10^8, and 1×10^8 PFU/mL) and curcumin suspension (400 µg/mL) simultaneously, and (iv) a double dose of both phage and curcumin suspension, administered at 0 and 1 h. A control treatment consisted of cultures of *A. baumannii* isolate 131 in LB broth. All treated cultures were incubated at either room temperature (25 °C) or 37 °C. At the indicated time points (1, 2, 3, 5, 6, 8, and 24 h) post-treatment, 1 mL of the cultures were sampled and viable bacteria and phages were enumerated as above compared with the initial number of bacteria (0 h).

Statistical analysis

Each experiment was performed in triplicate and the data analyzed using GraphPad Prism software and presented as mean ± standard deviation (mean ± SD). The Student's *t*-test was used to compare means between treated and untreated groups, while one-way analysis of variance (ANOVA) was used to compare means across three or more groups. Statistical significance was considered when the *p*-value was less than 0.05 (* $P < 0.05$, ** $P < 0.01$, *** $P < 0.001$, **** $P < 0.0001$, ns; not significant). Independent experiments were repeated three times.

Data availability

Whole genome sequence of vB_AbaSI_1 was deposited in the GenBank database under accession number PP359530 (https://www.ncbi.nlm.nih.gov/nuccore/PP359530).

Received: 11 December 2024; Accepted: 11 March 2025
Published online: 15 March 2025

References

1. Organization, W. H. February. WHO publishes list of bacteria for which new antibiotics are urgently needed. 27 ed. (2017). https://www.who.int/news/item/27-02-2017-who-publishes-list-of-bacteria-for-which-new-antibiotics-are-urgently-needed; 2017.
2. GBD 2021 Antimicrobial Resistance Collaborators. Global burden of bacterial antimicrobial resistance 1990–2021: A systematic analysis with forecasts to 2050. *Lancet* **404**, 10459 (2024).
3. Teerawattanapong, N. et al. A systematic review of the burden of multidrug-resistant healthcare-associated infections among intensive care unit patients in Southeast Asia: The rise of multidrug-resistant *Acinetobacter baumannii*. *Infect. Control Hosp. Epidemiol.* **39**, 525–533 (2018).
4. Lim, C. et al. Epidemiology and burden of multidrug-resistant bacterial infection in a developing country. *Elife* **5** (2016).
5. Loraine, J. et al. Genomic and phenotypic analyses of *Acinetobacter baumannii* isolates from three tertiary care hospitals in Thailand. *Front. Microbiol.* **11**, 548 (2020).
6. Prevention, C. f.D.C.a. COVID-19: U.S. impact on antimicrobial resistance, special report 2022. Atlanta, GA. Published June 2022. Accessed 10 January 2023.
7. Elfadadny, A. R. et al. Exploring bacteriophage applications in medicine and beyond. *Acta Microbiol. Hellenica*. **69**, 167–179 (2024).
8. Choi, Y. J., Kim, S., Shin, M. & Kim, J. Synergistic antimicrobial effects of phage vB_AbaSi_W9 and antibiotics against *Acinetobacter baumannii* infection. *Antibiot. (Basel)* **13** (2024).
9. Rastegar, S. et al. Synergistic effects of bacteriophage cocktail and antibiotics combinations against extensively drug-resistant *Acinetobacter baumannii*. *BMC Infect. Dis.* **24**, 1208 (2024).
10. Plumet, L., Costechareyre, D., Lavigne, J. P., Kissa, K. & Molle, V. Zebrafish as an effective model for evaluating phage therapy in bacterial infections: A promising strategy against human pathogens. *Antimicrob. Agents Chemother.* **68**, e0082924 (2024).
11. Shivaswamy, V. C. et al. Ability of bacteriophage in resolving wound infection caused by multidrug-resistant *Acinetobacter baumannii* in uncontrolled diabetic rats. *Microb. Drug Resist.* **21**, 171–177 (2015).
12. Hua, Y. et al. Phage therapy as a promising new treatment for lung infection caused by carbapenem-resistant *Acinetobacter baumannii* in mice. *Front. Microbiol.* **8**, 2659 (2017).
13. Ambroa, A. et al. Genomic analysis of molecular bacterial mechanisms of resistance to phage infection. *Front. Microbiol.* **12**, 784949 (2021).
14. Grygorcewicz, B. et al. Antibiotics act with vB_AbaP_AGC01 phage against *Acinetobacter baumannii* in human heat-inactivated plasma blood and *Galleria Mellonella* models. *Int. J. Mol. Sci.* **21** (2020).
15. Nir-Paz, R. et al. Successful treatment of antibiotic-resistant, poly-microbial bone infection with bacteriophages and antibiotics combination. *Clin. Infect. Dis.* **69**, 2015–2018 (2019).
16. Pimchan, T., Cooper, C. J., Eumkeb, G. & Nilsson, A. S. *In vitro* activity of a combination of bacteriophages and antimicrobial plant extracts. *Lett. Appl. Microbiol.* **66**, 182–187 (2018).
17. Wintachai, P. & Voravuthikunchai, S. P. Characterization of novel lytic myoviridae phage infecting multidrug-resistant *Acinetobacter baumannii* and synergistic antimicrobial efficacy between phage and Sacha Inchi oil. *Pharmaceuticals (Basel)* 15 (2022).
18. Prasad, S. & Aggarwal, B. B. Turmeric, the golden Spice: from traditional medicine to modern medicine. In Benzie, I. F. F. & Wachtel-Galor, S. (eds) *Herbal Medicine: Biomolecular and Clinical Aspects*, 2nd edn. (2011).
19. Goel, A., Kunnumakkara, A. B. & Aggarwal, B. B. Curcumin as Curecumin: From kitchen to clinic. *Biochem. Pharmacol.* **75**, 787–809 (2008).
20. Tripathy, S. et al. Curcumin extraction, isolation, quantification and its application in functional foods: A review with a focus on immune enhancement activities and COVID-19. *Front. Nutr.* **8**, 747956 (2021).
21. Gera, M. et al. Nanoformulations of Curcumin: An emerging paradigm for improved remedial application. *Oncotarget* **8**, 66680–66698 (2017).
22. Tung, B. T., Nham, D. T., Hai, N. T. & Thu, D. K. Chapter 10 - curcuma longa, the polyphenolic curcumin compound and pharmacological effects on liver. In Watson, R. R. & Preedy, V. R. (eds) *Dietary Interventions in Liver Disease*. Academic, 125–134. (2019).
23. Zhang, J., Zhang, R., Jin, S. & Feng, X. Curcumin, a plant polyphenol with multiple physiological functions of improving antioxidation, anti-inflammation, immunomodulation and its application in poultry production. *J. Anim. Physiol. Anim. Nutr. (Berl).* **108**, 1890–1905 (2024).
24. Aggarwal, B. B. & Harikumar, K. B. Potential therapeutic effects of Curcumin, the anti-inflammatory agent, against neurodegenerative, cardiovascular, pulmonary, metabolic, autoimmune and neoplastic diseases. *Int. J. Biochem. Cell. Biol.* **41**, 40–59 (2009).
25. Panahi, Y. et al. Effects of Curcumin on serum cytokine concentrations in subjects with metabolic syndrome: A post-hoc analysis of a randomized controlled trial. *Biomed. Pharmacother.* **82**, 578–582 (2016).
26. Kuptniratsaikul, V. et al. Efficacy and safety of *Curcuma domestica* extracts compared with ibuprofen in patients with knee osteoarthritis: A multicenter study. *Clin. Interv Aging.* **9**, 451–458 (2014).
27. Gupta, S. C., Patchva, S. & Aggarwal, B. B. Therapeutic roles of Curcumin: Lessons learned from clinical trials. *AAPS J.* **15**, 195–218 (2013).
28. Dai, C. et al. The natural product Curcumin as an antibacterial agent: Current achievements and problems. *Antioxid. (Basel)* 11 (2022).
29. Raorane, C. J. et al. Antibiofilm and antivirulence efficacies of flavonoids and Curcumin against *Acinetobacter baumannii*. *Front. Microbiol.* **10**, 990 (2019).
30. Chung, K. M., Liau, X. L. & Tang, S. S. Bacteriophages and their host range in multidrug-resistant bacterial disease treatment. *Pharmaceuticals (Basel)* **16** (2023).
31. Nasr-Eldin, M. A., Gamal, E., Hazza, M. & Abo-Elmaaty, S. A. Isolation, characterization, and application of lytic bacteriophages for controlling *Enterobacter cloacae* complex (ECC) in pasteurized milk and yogurt. *Folia Microbiol. (Praha).* **68**, 911–924 (2023).
32. Stojkovic, E. A. & Rothman-Denes, L. B. Coliphage N4 N-acetylmuramidase defines a new family of murein hydrolases. *J. Mol. Biol.* **366**, 406–419 (2007).
33. Dedrick, R. M. et al. Engineered bacteriophages for treatment of a patient with a disseminated drug-resistant *Mycobacterium abscessus*. *Nat. Med.* **25**, 730–733 (2019).
34. Perez-Arellano, I., Rubio, V. & Cervera, J. Dissection of *Escherichia coli* glutamate 5-kinase: Functional impact of the deletion of the PUA domain. *FEBS Lett.* **579**, 6903–6908 (2005).
35. Paulin, K. A., Cortez, D. & Eichman, B. F. The SOS response-associated peptidase (SRAP) domain of YedK catalyzes ring opening of Abasic sites and reversal of its DNA-protein cross-link. *J. Biol. Chem.* **298**, 102307 (2022).
36. Yao, J. et al. Type II toxin/antitoxin system ParE(SO) /CopA(SO) stabilizes prophage CP4So in *Shewanella oneidensis*. *Environ. Microbiol.* **20**, 1224–1239 (2018).
37. Sattar, S. et al. Characterization of two novel lytic bacteriophages having Lysis potential against MDR avian pathogenic *Escherichia coli* strains of zoonotic potential. *Sci. Rep.* **13**, 10043 (2023).
38. Oechslin, F. Resistance development to bacteriophages occurring during bacteriophage therapy. *Viruses* **10** (2018).
39. Gummalla, V. S., Zhang, Y., Liao, Y. T. & Wu V.C.H. The role of temperate phages in bacterial pathogenicity. *Microorganisms* **11** (2023).

40. Tenorio-Carnalla, K. et al. Host population structure and species resolution reveal prophage transmission dynamics. *mBio* **15**, e0237724 (2024).
41. Touchon, M., Bernheim, A. & Rocha, E. P. Genetic and life-history traits associated with the distribution of prophages in bacteria. *ISME J.* **10**, 2744–2754 (2016).
42. Knecht, L. E., Veljkovic, M. & Fieseler, L. Diversity and function of phage encoded depolymerases. *Front. Microbiol.* **10**, 2949 (2019).
43. Khan, F. M. et al. A novel *Acinetobacter baumannii* bacteriophage endolysin LysAB54 with high antibacterial activity against multiple Gram-negative microbes. *Front. Cell. Infect. Microbiol.* **11**, 637313 (2021).
44. Oliveira, H. et al. Functional analysis and antivirulence properties of a new depolymerase from a myovirus that infects *Acinetobacter baumannii* capsule K45. *J. Virol.* **93** (2019).
45. Popova, A. V. et al. Characterization of myophage AM24 infecting *Acinetobacter baumannii* of the K9 capsular type. *Arch. Virol.* **164**, 1493–1497 (2019).
46. Jiang, L. et al. Isolation and characterization of a novel myophage Abp9 against pandrug resistant *Acinetobacater baumannii*. *Front. Microbiol.* **11**, 506068 (2020).
47. Lai, M. J. et al. The tail associated protein of *Acinetobacter baumannii* phage phiAB6 is the host specificity determinant possessing exopolysaccharide depolymerase activity. *PLoS ONE*. **11**, e0153361 (2016).
48. Margulieux, K. R. et al. Complete genome sequence of the broad host range *Acinetobacter baumannii* phage EAb13. *Microbiol. Resour. Announc*. **12**, e0034123 (2023).
49. Labrie, S. J., Samson, J. E. & Moineau, S. Bacteriophage resistance mechanisms. *Nat. Rev. Microbiol.* **8**, 317–327 (2010).
50. Kortright, K. E., Chan, B. K., Koff, J. L. & Turner, P. E. Phage therapy: A renewed approach to combat antibiotic-resistant bacteria. *Cell. Host Microbe*. **25**, 219–232 (2019).
51. Chan, B. K., Abedon, S. T. & Loc-Carrillo, C. Phage cocktails and the future of phage therapy. *Future Microbiol.* **8**, 769–783 (2013).
52. Jia, H. J. et al. Engineering bacteriophages for enhanced host range and efficacy: Insights from bacteriophage-bacteria interactions. *Front. Microbiol.* **14**, 1172635 (2023).
53. van den Berg, D. F., van der Steen, B. A., Costa, A. R. & Brouns, S. J. J. Phage tRNAs evade tRNA-targeting host defenses through anticodon loop mutations. *Elife* **12** (2023).
54. Kali, A., Bhuvaneshwar, D., Charles, P. M. & Seetha, K. S. Antibacterial synergy of curcumin with antibiotics against biofilm producing clinical bacterial isolates. *J. Basic. Clin. Pharm.* **7**, 93–96 (2016).
55. Varshney, G. K., Saini, R. K., Gupta, P. K. & Das, K. Effect of Curcumin on the diffusion kinetics of a hemicyanine dye, LDS-698, across a lipid bilayer probed by second harmonic spectroscopy. *Langmuir* **29**, 2912–2918 (2013).
56. Rai, D., Singh, J. K., Roy, N. & Panda, D. Curcumin inhibits FtsZ assembly: An attractive mechanism for its antibacterial activity. *Biochem. J.* **410**, 147–155 (2008).
57. Sethupathy, S. et al. Proteomic analysis reveals modulation of iron homeostasis and oxidative stress response in *Pseudomonas aeruginosa* PAO1 by Curcumin inhibiting quorum sensing regulated virulence factors and biofilm production. *J. Proteom.* **145**, 112–126 (2016).
58. Marathe, S. A., Ray, S. & Chakravortty, D. Curcumin increases the pathogenicity of *Salmonella enterica* serovar typhimurium in murine model. *PLoS ONE*. **5**, e11511 (2010).
59. Zheng, D. et al. Antibacterial mechanism of Curcumin: A review. *Chem. Biodivers.* **17**, e2000171 (2020).
60. Murai, H. et al. Curcumin inhibits growth of *Porphyromonas gingivalis* by arrest of bacterial dipeptidyl peptidase activity. *J. Oral Microbiol.* **16**, 2373040 (2024).
61. McConnell, M. J., Actis, L. & Pachon, J. *Acinetobacter baumannii*: Human infections, factors contributing to pathogenesis and animal models. *FEMS Microbiol. Rev.* **37**, 130–155 (2013).
62. Liu, C. H. & Huang, H. Y. Antimicrobial activity of curcumin-loaded myristic acid microemulsions against *Staphylococcus epidermidis*. *Chem. Pharm. Bull. (Tokyo)*. **60**, 1118–1124 (2012).
63. Oliveira, P. H., Touchon, M. & Rocha, E. P. The interplay of restriction-modification systems with mobile genetic elements and their prokaryotic hosts. *Nucleic Acids Res.* **42**, 10618–10631 (2014).
64. Lucidi, M. et al. Phage-mediated colistin resistance in *Acinetobacter baumannii*. *Drug Resist. Updat.* **73**, 101061 (2024).
65. Withatanung, P. et al. Induced *Burkholderia* prophages detected from the hemoculture: A biomarker for *Burkholderia Pseudomallei* infection. *Front. Microbiol.* **15**, 1361121 (2024).
66. Nale, J. Y. et al. Bacteriophage combinations significantly reduce *Clostridium difficile* growth *in vitro* and proliferation *in vivo*. *Antimicrob. Agents Chemother.* **60**, 968–981 (2016).
67. Kropinski, A. M. Practical advice on the one-step growth curve. *Methods Mol. Biol.* **1681**, 41–47 (2018).
68. Nishimura, Y. et al. ViPTree: The viral proteomic tree server. *Bioinformatics* **33**, 2379–2380 (2017).
69. Gilchrist, C. L. M. & Chooi, Y. H. Clinker & Clustermap.js: Automatic generation of gene cluster comparison figures. *Bioinformatics* **37**, 2473–2475 (2021).
70. Wang, R. H. et al. PhageScope: A well-annotated bacteriophage database with automatic analyses and visualizations. *Nucleic Acids Res.* **52**, D756–D761 (2024).
71. Kutter, E. Phage host range and efficiency of plating. *Methods Mol. Biol.* **501**, 141–149 (2009).

Acknowledgements

The researchers wish to express their deepest gratitude to Dr. Vanaporn Wuthiekanun (Mahidol-Oxford Tropical Medicine Research Unit, Mahidol University) and Miss Natnaree Saiprom (Faculty of Tropical Medicine, Mahidol University) for bacterial isolation in this study.

Author contributions

Conceptualization: SK and PW Data curation: SJ, SK and PW. Formal analysis: SJ, TS, SK and PW. Funding acquisition: SK. Investigation: SJ, TS, VM, MV, OG, JYN and PW. Methodology: SJ, TS, SK and PW. Project administration: SJ, SK and PW. Resources: PS, KK and NC. Software: OG. and PW. Supervision: SK and PW. Validation: SK and PW. Writing - original draft: SJ, JYN, SK and PW. All authors reviewed and approved the final manuscript.

Funding

This research project was financial supported by the Agricultural Research Development Agency (Public Organization) of Thailand or "ARDA" (PRP6605031640). SK, PW, VM, TS and SJ were supported by the Siriraj Research and Development Fund, Faculty of Medicine Siriraj Hospital, Mahidol University, Thailand.

Declarations

Competing interests
The authors declare no competing interests.

Additional information
Supplementary Information The online version contains supplementary material available at https://doi.org/10.1038/s41598-025-94040-y.

Correspondence and requests for materials should be addressed to P.W.

Reprints and permissions information is available at www.nature.com/reprints.

Publisher's note Springer Nature remains neutral with regard to jurisdictional claims in published maps and institutional affiliations.